

**New Results on Particle and Astroparticle
Physics with an Emphasis on Higgs
Physics**

Peter Fackeldey, RWTH Aachen University

Abstract

In July 2012 the two experiments CMS [1] and ATLAS [2] observed a new particle, namely the Higgs boson. The discovery in the decay channels $H \rightarrow ZZ$ and $H \rightarrow \gamma\gamma$ marks a keystone in particle physics. The last missing piece of the Standard Model of particle physics was found and validates the existence of the so-called Higgs field predicted by Peter Higgs in 1964 [3, 4]. This write up describes the fundamental principles of Higgs physics and the discovery of the consequently predicted Higgs boson. Special insight is given into the $H \rightarrow ZZ \rightarrow 4\ell$ analysis, the famous "golden channel", which provides the highest precision for measuring the mass of the Higgs boson.

Contents

Introduction	1
1 The Standard Model of Particle Physics	3
1.1 Proton-proton Collisions at LHC	4
1.2 The Higgs Mechanism and Its Consequences	5
1.2.1 EBH Mechanism and the Higgs boson	5
1.2.2 Yukawa Interaction	6
1.2.3 Properties of the Higgs Boson	7
2 Higgs Searches	11
2.1 Higgs Discovery	11
2.2 Golden Channel: $H \rightarrow ZZ \rightarrow 4\ell$	13
2.3 Recent $H \rightarrow \tau\tau$ Discovery	15
3 Conclusion	17
3.1 Measurements of the Properties of the Higgs Boson	17
3.2 Exciting Times Ahead...	19
Bibliography	21

Introduction

The Standard Model (SM) of particle physics [5–7] has proven to describe elementary particles and their interactions successfully. The model separates between fermions (spin 1/2) and bosons (integer spin) particles. The bosons function as mediators of the fundamental forces of the SM. Fermions are further subdivided into quarks and leptons. Quarks are taking part in the strong interaction. The u and d quark and their antiparticle partners form together with 8 different gluons (mediators of the strong interaction) the nuclei of atoms. Leptons, such as electrons, are mainly interacting via electroweak interaction. The bosons of the electroweak interaction are γ , Z and W^\pm (weak gauge bosons).

The biggest problem of the SM is that it does not contain mass terms for all massive particles, especially the Z and W^\pm bosons. Unfortunately this problem can not be solved by adding new mass terms to the SM lagrangian without losing gauge invariance. Since the SM provides such accurate predictions for the properties of all elementary particles and their interactions, a lot of effort was made by theorists in the 60s to save this model by adding a new mechanism, the so-called Higgs mechanism. The mechanism itself was introduced by a couple of theorists: R. Brout, F. Englert, P. Higgs, G. S. Guralnik, C. R. Hagen, and T. W. B. Kibble. Francois Englert and Peter Higgs were awarded with the nobel prize in 2013. The next chapter describes the SM, the Higgs mechanism and its resulting consequences.

The Standard Model of Particle Physics

Four fundamental forces are known up to know: the electromagnetic force, the weak force, the strong force and the gravitational force. The first three forces are well described within the SM, while the latter can be described by general relativity. For all these interactions, except of the gravitational force, an unique quantum field theory is existing. The interactions are mediated by gauge bosons. The SM in its full magnificence is represented by a gauge group of the form $SU(3)_C \times SU(2)_L \times U(1)_Y$, where the indices correspond to the color charge C , the weak isospin L and the weak hypercharge Y . The $SU(3)_C$ gauge group describes the quantum chromodynamics (QCD), which force (strong force) couples to three color charges (red, green or blue). Demanding local gauge symmetry within the QCD lagrangian 8 gauge bosons are predicted for the strong force, namely gluons with different color charge. The weak and electromagnetic force can be unified to the electroweak force, which is described by the gauge group $SU(2)_L \times U(1)_Y$. The physical gauge bosons of this unification appear, mixing the abstract fields B and W_3 with a rotation matrix parametrized by the weak mixing angle θ_W and combining the fields W_1 and W_2 : the photon γ , the Z boson Z^0 and the two charged W bosons W^\pm . All gauge bosons are listed in the following table.

Table 1.1: Gauge bosons

Interaction	Gauge Boson	Mass / GeV
electromagnetic	Photon γ	0
weak	Z^0	91.18
	W^\pm	80.40
strong	8 Gluons g	0

The remaining fundamental particles are fermions. As described in the introduction they are subdivided into leptons and quarks. A full list of fermions are given below.

Table 1.2: Left-handed elementary fermions. Right-handed elementary fermions do not carry any weak isospin.

Fermions	Generation			Charge		
	1	2	3	El. Charge	Weak Isospin	Colour
Leptons	ν_e	ν_μ	ν_τ	0	$+\frac{1}{2}$	0
	e	μ	τ	$-e$	$-\frac{1}{2}$	
Quarks	u	c	t	$+\frac{2}{3}e$	$+\frac{1}{2}$	red, green, blue
	d	s	b	$-\frac{1}{3}e$	$-\frac{1}{2}$	

1.1 Proton-proton Collisions at LHC

QCD plays an important role at LHC, since it is a proton-proton collider. The protons are accelerated up to a center-of-mass energy of $\sqrt{s} = 7 - 8\text{TeV}$ in Run 1 and up to $\sqrt{s} = 13\text{TeV}$ since Run 2. However protons constitute of much smaller particles: quarks and gluons. To be more precise a proton consists of three valence quarks: two u quarks and one d quark. Furthermore it contains so-called sea quarks and gluons. The total center-of-mass energy is therefore divided between all subparticles of the proton (partons). The following two figures show the parton distribution functions (PDFs) multiplied by the momentum fraction x for the different partons.

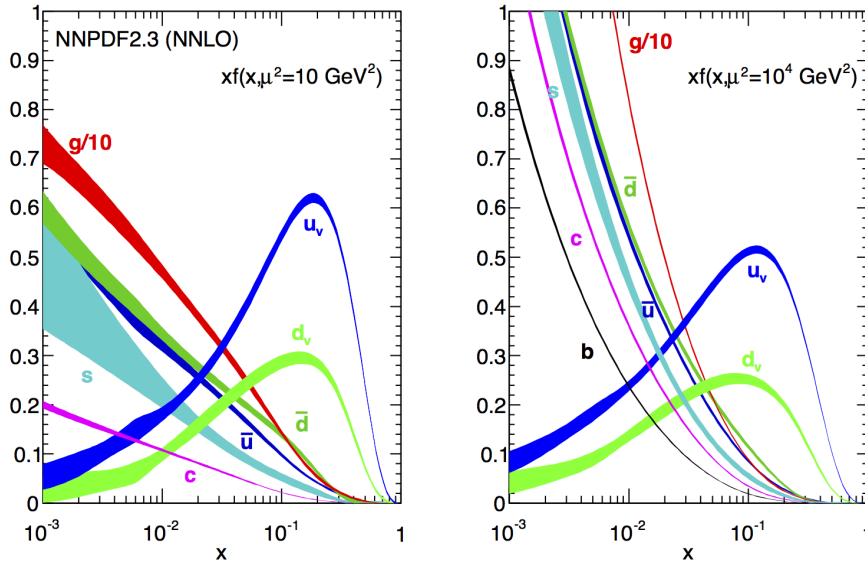


Figure 1.1: Parton distribution functions of the the NNPDF Collaboration for two different energy scales [8]. The x-axis denotes the momentum fraction x carried by the valence quarks, the sea quarks and gluons.

Collisions at LHC take place between two quarks, two gluons or a quark and a gluon. Therefore the real center-of-mass energy at each collision, paying respect to the PDFs, is unknown. Since the partons of the proton are strongly interacting, QCD processes will play a huge role for all hard-scattering processes, especially the search for the SM Higgs boson.

1.2 The Higgs Mechanism and Its Consequences

1.2.1 EBH Mechanism and the Higgs boson

As already mentioned before, the SM is lacking mass terms in the lagrangian. In order to keep the SM lagrangian renormalizable one has to demand gauge invariance. Artificially introducing mass terms to the SM lagrangian violates this fundamental principle. Therefore a new mechanism has to be introduced by which the weak gauge bosons gain their mass.

A new scalar field ϕ is introduced. This scalar doublet reads:

$$\phi = \begin{pmatrix} \phi^+ \\ \phi^0 \end{pmatrix} = \frac{1}{\sqrt{2}} \begin{pmatrix} \phi_1 + i\phi_2 \\ \phi_3 + i\phi_4 \end{pmatrix} \quad (1.1)$$

A lagrangian based on this field can be constructed, containing a term for the kinetic energy and one for the potential energy.

$$\mathcal{L}_{\text{Higgs}} = \underbrace{(D^\mu \Phi)^\dagger (D_\mu \Phi)}_{\text{Kinetic}} - \underbrace{\mu^2 \Phi^\dagger \Phi - \lambda (\Phi^\dagger \Phi)^2}_{\text{Potential}} \quad (1.2)$$

The potential contains two parameters: λ and μ^2 . The first parameter is real and positive and describes a self coupling term. The other term, containing μ^2 , looks already like a mass-type term. If μ^2 is chosen to be positive, there is only one ground state possible: $\langle \Phi \rangle_{\min} = 0$. But this will not solve the aforementioned mass problem. Choosing μ^2 to be negative leads to the following minimum of the potential:

$$\frac{\partial V}{\partial \Phi^\dagger \Phi} = \mu^2 + 2\lambda \Phi^\dagger \Phi \quad (1.3)$$

$$\Rightarrow |\Phi_{\min}| = \sqrt{\frac{-\mu^2}{2\lambda}} = \frac{v}{\sqrt{2}}, \quad (1.4)$$

where v denotes the vacuum expectation value (VEV). Without the loss of generality the fields $\Phi_i, i = 1..4$ can be chosen in the following way:

$$\Phi_1 = \Phi_2 = \Phi_4 = 0 \quad \text{and} \quad \Phi_3 = \Phi_{\min} \quad (1.5)$$

Now the ground state of the potential is no longer symmetric under SU(2) rotations, but still keeping the renormalizability, which was shown in 1972 [9]. This choice leads to a ground state which can be

expanded by using the Higgs field $h(x)$:

$$\langle \Phi \rangle_0 = \frac{1}{\sqrt{2}} \begin{pmatrix} 0 \\ v \end{pmatrix} \Rightarrow \Phi(x) = \frac{1}{\sqrt{2}} \begin{pmatrix} 0 \\ v + h(x) \end{pmatrix} \quad (1.6)$$

With $\Phi(x)$ one can expand $\mathcal{L}_{\text{Higgs}}$ 1.2. The kinetic term $|D_\mu \Phi|^2$ reads:

$$|D_\mu \Phi|^2 = \frac{1}{8} v^2 g_2^2 |W_\mu^1 + i W_\mu^2|^2 + \frac{1}{8} v^2 |g_2 W_\mu^3 - g_1 B_\mu|^2 + \dots \quad (1.7)$$

$$= \frac{1}{2} m_W^2 W_\mu^+ W_\mu^- + \frac{1}{2} m_Z^2 Z_\mu Z^\mu + 0 \cdot A_\mu A^\mu \quad (1.8)$$

Here v denotes the VEV, g the coupling constant and $W_\mu^{1,2,3}$ and B_μ the gauge fields of the electroweak theory. W_μ^\pm , Z_μ and A_μ are the physical representations of these gauge fields. Finally one can see that the kinetic term directly rises mass terms for the weak gauge bosons, but not for the photon. The same expansion can be done for the potential of the Higgs lagrangian:

$$V = \frac{1}{2} \mu^2 (v + H)^2 + \frac{1}{4} \lambda (v + H)^4 \Rightarrow m_H = -\sqrt{2} \mu = v \sqrt{2 \lambda} \quad (1.9)$$

A very interesting property of the Higgs field appears: It comes along with a new particle with the mass $m_H = v \sqrt{2 \lambda}$, the SM Higgs boson. Additionally one can see trilinear and quartic self-coupling terms in the expansion of the potential.

All in all a mechanism is introduced, which spontaneously breaks the SU(2) symmetry, but not the U(1) or SU(3) symmetry. This leads to mass terms for the weak gauge bosons, but not for the photon or the gluon, while keeping the SM lagrangian renormalizable.

1.2.2 Yukawa Interaction

In order to generate mass to the fermions, using the same principle as before, Yukawa interaction terms are added to the lagrangian. Yukawa interaction describes the interaction between a scalar field (Higgs field) and a Dirac field (fermion field). Additionally one has to pay respect to the chirality of the fermions. The lagrangian for the fermion mass then reads:

$$\mathcal{L}_{\text{mf}} = -\lambda_f (\psi_L^\dagger \Phi \psi_R + \psi_R^\dagger \Phi^\dagger \psi_L) \quad \text{with} \quad \Phi(x) = \frac{1}{\sqrt{2}} \begin{pmatrix} 0 \\ v + H(x) \end{pmatrix} \quad (1.10)$$

Here ψ_L describes the left-handed doublet and ψ_R the right-handed singlet. After spontaneous symmetry breaking the fermion mass m_f and the coupling to the Higgs field g_{Hff} appear:

$$m_f = \frac{v}{2} \lambda_f \quad \text{and} \quad g_{Hff} = \frac{m_f}{v} \quad (1.11)$$

This principle now also generates mass for the fermions. Finally one can conclude from the coupling to the Higgs field, that the coupling strength is proportional to the fermion mass.

1.2.3 Properties of the Higgs Boson

The Higgs boson differs from all other fundamental particles, since it has spin 0. It also is electrically neutral and does not carry any color charge. Its CP eigenvalue is predicted to be +1 and the only eigenvalue of the Higgs boson, which is not measured up to now.

In the past 50 years two accelerators were built with the main goal to find the Higgs boson. The first was the LEP accelerator, which was a electron-positron collider. Unfortunately it was not able to discover the Higgs boson, but strong exclusion limits could be set. Afterwards the LHC was built using the LEP tunnel. The LHC is a proton-proton collider running on high center-of-mass energies, which makes it a "discovery machine" and able to finally discover the Higgs boson. The relevant Higgs production feynman diagrams for such a machine are shown in figure 1.2.

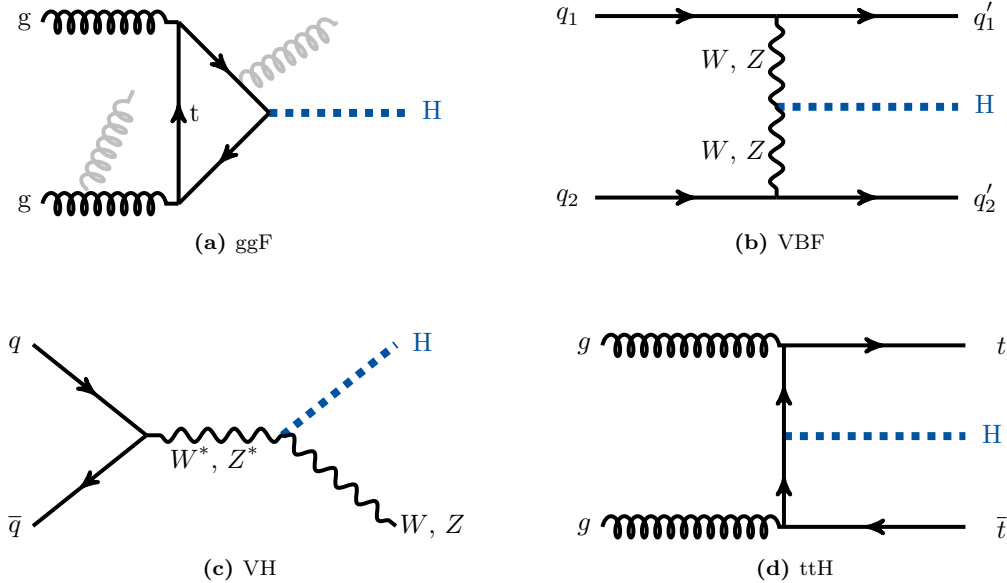


Figure 1.2: Feynman diagrams of the four main Higgs production modes at LHC.

The gluon fusion process (ggF) 1.2a is the most dominant production process at LHC. Two gluons produce a top loop, which couples to the Higgs boson. The loop can be produced by any quark, but it was shown before, that the fermion mass is proportional to the coupling to the Higgs boson. This makes the heaviest fermion the most probable to participate in this loop: the top quark. As shown in the feynman diagram jets can be radiated of the gluons or the loop causing a phenomena called initial state radiation (ISR). The radiation of jets boosts the Higgs boson, which can be exploited in Higgs searches, but also reduces the cross section of this Higgs production.

The second most prominent process is vector boson fusion (VBF) 1.2b. Two quarks radiate weak gauge bosons, which annihilate and produce a Higgs boson. The two quarks are then scattered into opposite directions, leading to a very clear detector signature of two forward jets.

The Higgs strahlung process (VH) 1.2c is suppressed at LHC since it requires the annihilation of two quarks. This process would be the most dominant at a proton-antiproton collider, such as Tevatron at

Fermilab. The annihilation produces an excited W^* or Z^* boson, which deexcites by radiating a Higgs boson.

The last remaining process is the top associated Higgs production (ttH) 1.2d. This process is highly suppressed, since it requires energies to produce two top quarks and a Higgs boson in the final state. It is neglected in most analysis.

Figure 1.3 shows the cross sections for the different Higgs productions and their total uncertainties at the LHC for two different center-of-mass energies as a function of the Higgs boson mass m_H .

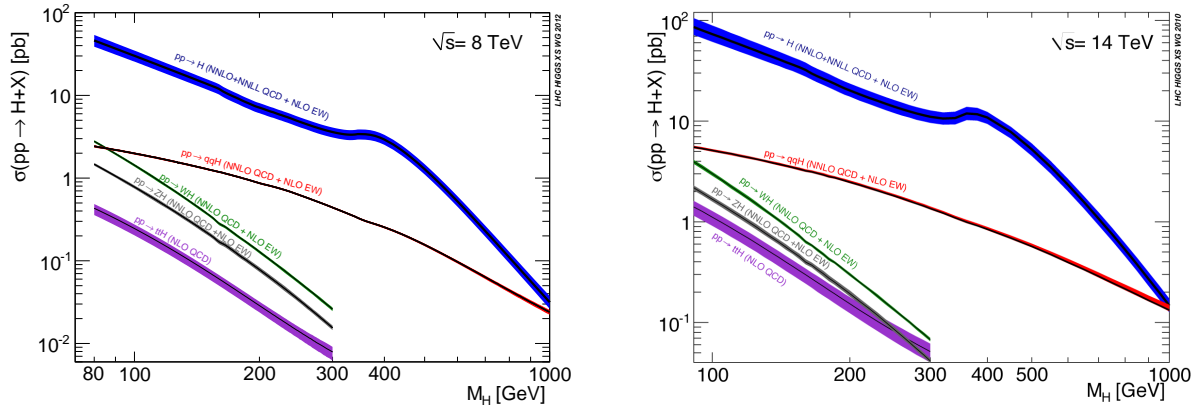


Figure 1.3: Predicted Higgs boson production cross sections for center-of-mass energies of $\sqrt{s} = 8$ TeV (left) and 14 TeV (right) [10–12].

From figure 1.3 one can conclude that the cross section decreases for increasing mass hypothesis. Here one can also see the relative differences in cross section for the four main production modes. As already said the gluon fusion process has the highest cross section, followed by the vector boson production mode. Here the difference in the cross section for a mass hypothesis of $m_H = 125$ GeV is approximately a factor of 10. For aforementioned reasons the cross sections for the Higgsstrahlung and the quark associated production mode are even smaller.

Since the Higgs boson has an extremely small lifetime, it will decay almost immediately in the detector. As a consequence one can only observe its decay products in the detector. The following figure 1.4 shows the branching fractions for different decay channels as a function of the mass hypothesis.

For low Higgs masses the branching fraction for a Higgs boson decaying into two heavy fermions (here b quark or τ lepton) is the largest, simply because its coupling is proportional to the fermion masses. The top quark mass is too large for this mass region of the Higgs boson. For higher mass hypothesis the decays to two W or Z bosons are dominating as soon as the Higgs boson mass surpasses the mass threshold for two on-shell W or Z bosons.

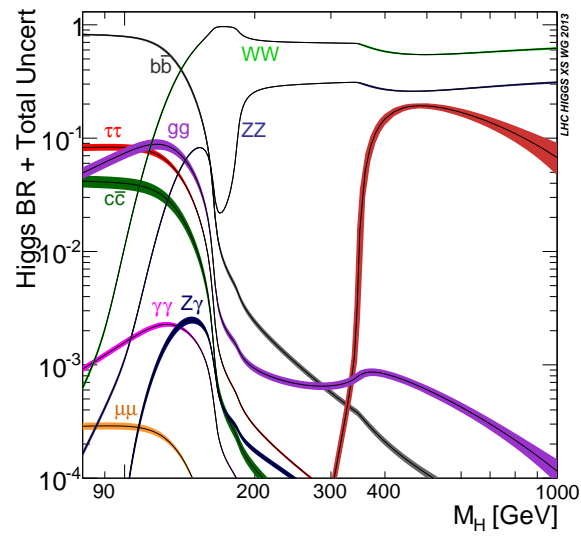


Figure 1.4: Predicted Higgs boson decay channel branching fractions as a function of the Higgs boson mass hypothesis [10–12].

Higgs Searches

2.1 Higgs Discovery

The experimental verification of the existence of a Higgs boson and therefore the Higgs mechanism was found by the two collaborations CMS and ATLAS in July 2012. The observation was found with a significance of 5.0σ (5.9σ) at a Higgs boson mass of approximately $m_H = 125$ GeV by CMS (ATLAS). It was necessary to combine different decay channel to achieve the observation with the measured LHC data of Run 1. Outstanding are the two golden channels $H \rightarrow ZZ \rightarrow 4\ell$ and $H \rightarrow \gamma\gamma$, which profit from a high mass resolution and controllable backgrounds. Figure 2.1 shows the discovery plots of both channel of the CMS collaboration.

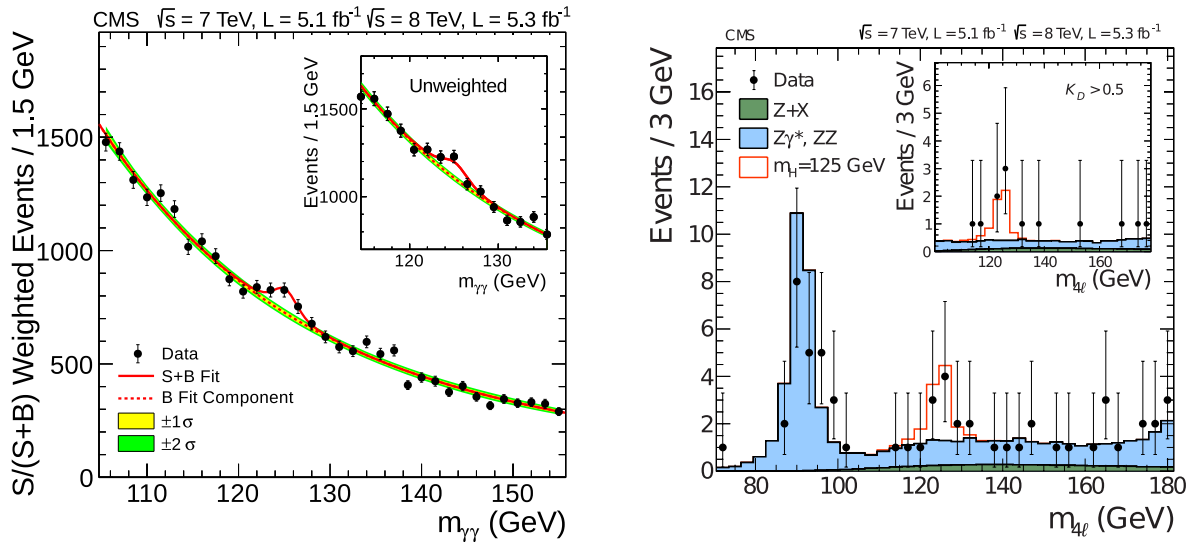


Figure 2.1: Higgs boson discoveries in the two golden channels $H \rightarrow \gamma\gamma$ (left) and $H \rightarrow ZZ \rightarrow 4\ell$ (right) by CMS [13].

Both discovery plots clearly show an excess in the invariant mass distribution at around $m_H = 125$ GeV. The left figure shows the invariant mass of two photons in a range between 100 GeV and 160 GeV.

The red dotted line shows the background only prediction (SM without Higgs boson) and the red line the signal plus background prediction (SM with Higgs boson). Also the 1σ and 2σ uncertainties are shown in a brazilian band style. The deviation show of the two hypothesis is clearly shown and is not compatible anymore within the uncertainties of the measured data.

The right figure shows the $H \rightarrow ZZ \rightarrow 4\ell$ channel. Here one can also see that the background only prediction can not explain any longer the measured data. The signal prediction of a Higgs boson with $m_H = 125$ is shown again in red and explains the excess in data very well. As a small example the basic analysis strategy is depicted in the following section 2.2.

Both decay channel leave a clear signature in the detector, which makes the reconstruction of the Higgs boson easier than in most other channel. Figure 2.2 shows two event displays corresponding to the two discovery plots from figure 2.1.

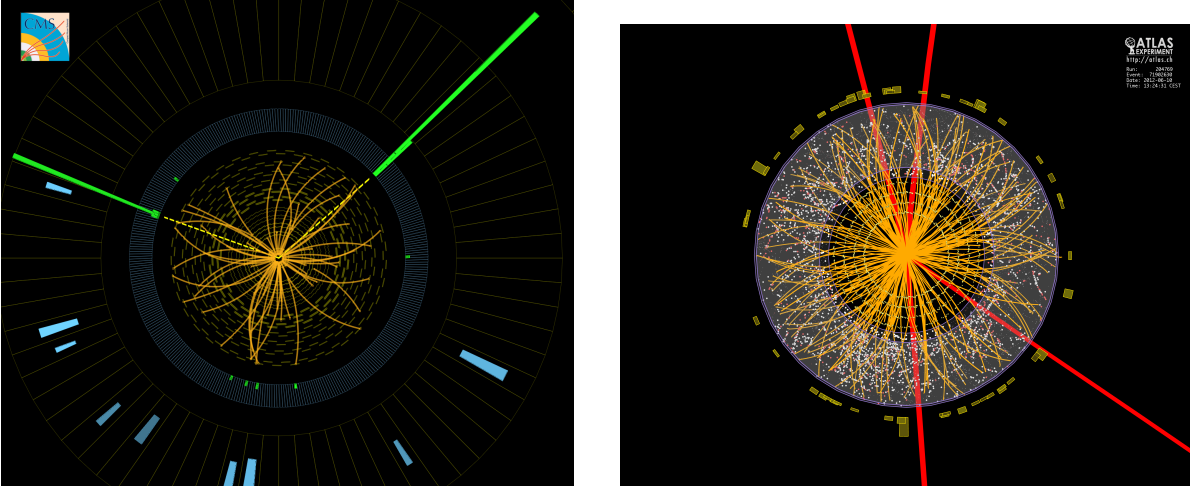


Figure 2.2: Higgs boson decay event displays in the two golden channels $H \rightarrow \gamma\gamma$ (left: CMS) and $H \rightarrow ZZ \rightarrow 4\ell$ (right: ATLAS).

In the left event display 2.2 one can clearly see entries in the electromagnetic calorimeter (ECAL) but not tracks (hinted with the dotted line). It is the signature of two photons, which interact electromagnetically (entries in ECAL) and have no electrically charge (no tracks). From the event display it is not possible to reconstruct the invariant mass, therefore it provides only the signatures in the detector for a Higgs boson candidate.

The right event display 2.2 shows four leptons in the detector. Furthermore one can specify them as muons, since they penetrate the whole detector complex. Unlike photons muons have an electrically charge and therefore leave a track in the inner tracker system of the detector. This event display also can only show a Higgs boson candidate, since the essential invariant mass information is missing.

In order to prove the observation of the Higgs boson statistical methods are needed. In fact it is a common strategy to perform hypothesis testing for the theory with and without the Higgs boson. They allow to quantify the compatibility between the SM with a Higgs boson and without a Higgs boson at a certain confidence level (usually chosen to be 95%). Figure 2.3 (left) shows the limit for a SM Higgs hypothesis as a function of different mass hypothesis. A clear excess of the data can be observed in

the mass interval of 120 GeV to 130 GeV. This means that one can not exclude a Higgs boson with $120 < m_H < 130$ GeV with the measured data of Run 1 from the SM.

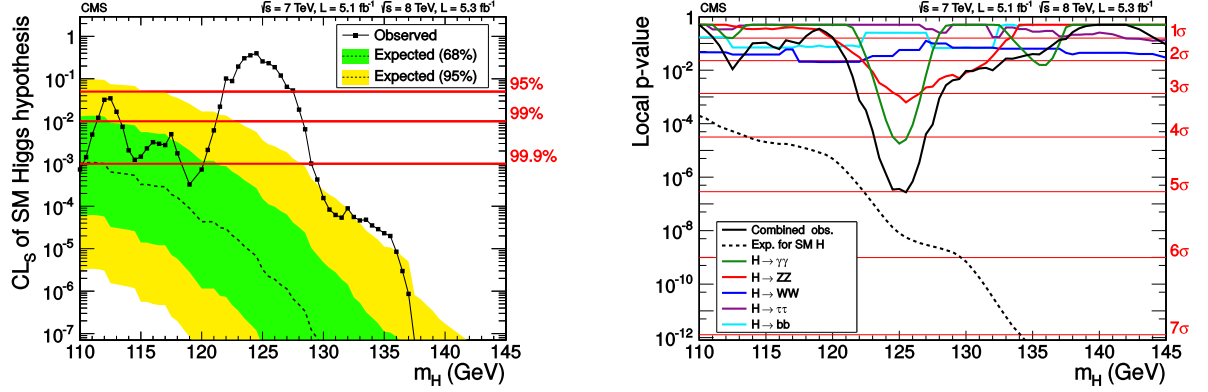


Figure 2.3: Expected and observed limit (left) and local p-value (right) as a function of different mass hypothesis [13].

Additionally it is possible to quantify the statistical significance of the measured excess. The local p-value is calculated as a function of the Higgs boson mass. From figure 2.3 (right) it is clear that the combined observed limit shows an excess of 5.0σ , making it a discovery. At the same time the best fit result for the Higgs mass can be extracted. It is measured to be:

- CMS: $m_H = 125.3 \pm 0.4$ (stat) ± 0.5 (sys) GeV [13]
- ATLAS: $m_H = 126.0 \pm 0.4$ (stat) ± 0.4 (sys) GeV [14]

Decay mode/combination	Expected (σ)	Observed (σ)
$\gamma\gamma$	2.8	4.1
ZZ	3.8	3.2
$\tau\tau + b\bar{b}$	2.4	0.5
$\gamma\gamma + ZZ$	4.7	5.0
$\gamma\gamma + ZZ + WW$	5.2	5.1
$\gamma\gamma + ZZ + WW + \tau\tau + b\bar{b}$	5.8	5.0

Figure 2.4: Table of expected and observed statistical significances for different decay channel [13].

The expected and observed significance for all analysed decay channels is depicted in table 2.4. It can be seen that including the $H \rightarrow \tau\tau$ and $H \rightarrow b\bar{b}$ the observed significance drops again. This was due to a bad statistical fluctuation in the measurement by CMS.

2.2 Golden Channel: $H \rightarrow ZZ \rightarrow 4\ell$

Although branching fraction of the $H \rightarrow ZZ \rightarrow 4\ell$ is quite small ($\approx 2.6\%$) it provides a very high mass resolution and a straight forward reconstruction of the Higgs boson. The basic analysis strategy is to

start with the four leptons, which are measured in the detector, and then reconstruct the Z bosons. Afterwards the two Z bosons can be combined to the Higgs boson.

As aforementioned one can only start this analysis by selecting four leptons. The possible combinations in this case are: $4e$, 4μ or $2e2\mu$. The tau leptons are neglected here, since their reconstruction efficiency is quite small in comparison to muons and electrons. The selection of the four leptons is done by introducing basic requirements. These cuts reject pile-up events (remnants from pp collisions), which one can see in the event displays from figure 2.2 as the yellow tracks.

Afterwards it is necessary to reconstruct Z boson candidates from the lepton selection. Two opposite sign same flavour leptons are combined. Their resulting invariant mass has to pass a mass window cut of $12 < m_{ll} < 120$ GeV. One of the combination is required to have the mass of the Z mass, since one Z boson is produced on-shell: $m_{ll} \approx m_Z$. The remaining two leptons are combined to a off-shell Z^* boson. For each event one can now combine the invariant mass of the four leptons of the ZZ^* selection in order to reconstruct the Higgs boson.

After the introduced event selection, the analysis has some remaining irreducible backgrounds. First of all there is the non-resonant ZZ and $Z\gamma^*$ process. From figure 2.5 it is obvious that they represent the main background of this analysis. The other irreducible background are merged into one background class, the so-called $Z + X$ process. This process is the combination of the following 5 background contributions: Z +jets, $t\bar{t}$ +jets, $Z\gamma$ +jets, WW +jets and WZ +jets. These processes do not leave four leptons in the detector, but instead the jets are misidentified as leptons by the reconstruction requirements. The rate of this is rather small, but non-negligible.

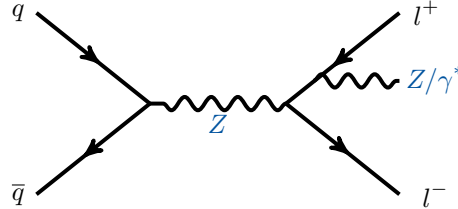


Figure 2.5: Feynman diagram of the non-resonant background ZZ and $Z\gamma^*$ in the $H \rightarrow ZZ \rightarrow 4\ell$ analysis.

This analysis was done again with Run 2 data. The Higgs boson was rediscovered, which marks a huge success. Figure 2.6 shows the rediscovery with data of $\mathcal{L} = 36.1$ taken in year 2016. A brand new (still on-going) analysis is currently at pre-approval. Therefore the signal region is still blinded in figure 2.7. Both plots show clearly an observed (expected) excess in data measured by ATLAS (CMS). Because of a higher integrated luminosity, the increase in center-of-mass energy from Run 1 to Run 2 and the improved analysis strategy, the excess in the four-lepton mass spectrum is larger than before.

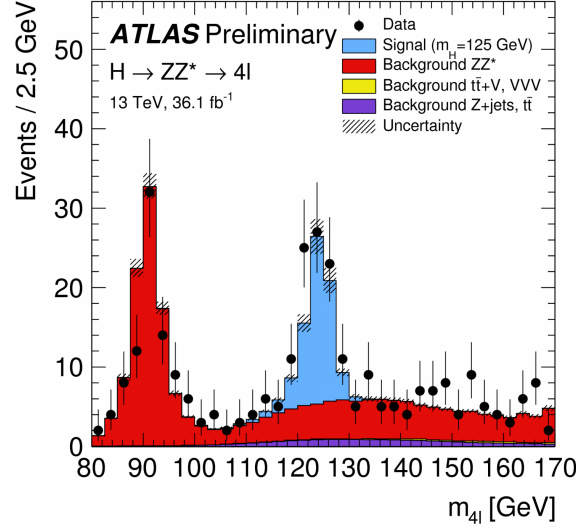


Figure 2.6: Higgs rediscovery in golden channel with 2016 data by ATLAS [15].

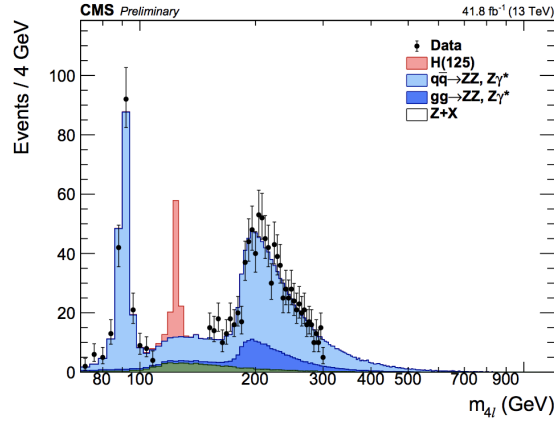


Figure 2.7: Brand new analysis with 2017 data by CMS [16] (right, still blinded)

2.3 Recent $H \rightarrow \tau\tau$ Discovery

In Run 1 the search for the SM Higgs boson decaying into a pair of tau leptons suffered from bad statistical fluctuations. Additionally this measurement is very challenging, since the reconstruction efficiency of tau leptons is rather bad in comparison to electrons and muons. Also this search has to deal with the QCD background, which is very hard to predict and badly modelled by Monte Carlo (MC) simulations.

Recently the decay of the SM Higgs boson into a pair of tau leptons could be observed by CMS. One of the most important approach in this analysis is to predict the QCD background from an exclusive region in data (not from MC). Using the ABCD method one is able to construct control regions for this background and therefore constrain the systematic uncertainty of the QCD cross-section. Additionally the analysis is splitted into different categories in order to enhance the sensitivity: 0-jet, VBF and

boosted category. Figure 2.8 shows the two discovery plots of the $H \rightarrow \tau\tau$ analysis. One can clearly see an excess in data in the invariant di-tau mass spectrum. This is especially visible in the "integrated" figure, where data minus background is shown. The statistical significance of the analysis is measured to be 5.9σ , making it a discovery. The best fit value for the SM Higgs boson signal strength is $\mu = 1.09^{+0.27}_{-0.26}$ at a Higgs boson mass of $m_H = 125.09$ GeV.

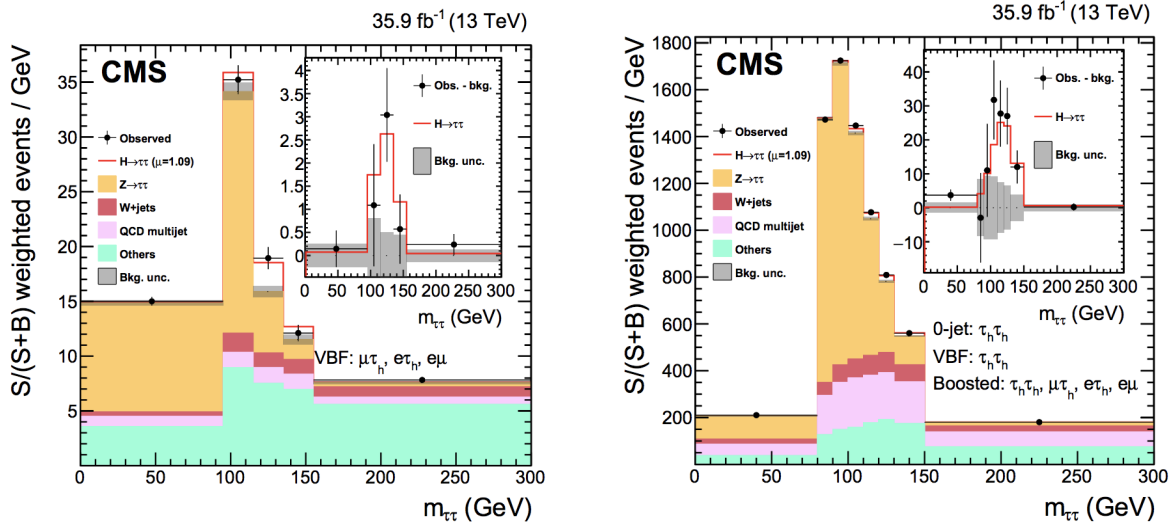


Figure 2.8: Discovery plots of a SM Higgs boson decaying into a pair of tau leptons. Left: Semi-leptonic decay channels. Right: Full-hadronic decay channel. [17].

3.1 Measurements of the Properties of the Higgs Boson

The collaborations CMS and ATLAS combined their measurements after Run 1 in order to measure the Higgs mass and the coupling to fermions with higher precision.

The combination of the Higgs mass was measured in the $H \rightarrow ZZ \rightarrow 4\ell$ and $H \rightarrow \gamma\gamma$ channel. A likelihood fit was performed in order to extract the best fit result for m_H from data. Figure 3.1 shows the likelihood parabola, where the minimum depicts the best fit value for m_H . Furthermore one can directly extract the 1σ (2σ) uncertainty from this plot by looking at the value for m_H for $-2\ln\Lambda(m_H) = 1$ (4). The best fit value for the Higgs mass was determined to be: $m_H = 125.09 \pm 0.21(\text{stat.}) \pm 0.11(\text{syst.})$ GeV.

As aforementioned the Higgs coupling was measured in a combined measurement. The coupling strength of the Higgs boson was predicted to be proportional to the mass of the fermions or vector bosons. It is shown in figure 3.2, that this predictions holds within the uncertainties of the data points. A deviation in data from this fit would already be a clear hint to something new. Therefore it is necessary to study all the SM Higgs boson decays with a very high precision.

By measuring the SM Higgs decaying into a pair of photons and a pair of tau leptons it is directly clear that the measured Higgs boson is a spin-0 particle and electrically neutral. Unfortunately the amount of data is still too low to measure the CP eigenvalue of the Higgs boson. The SM Higgs is predicted to have a CP eigenvalue of +1. A deviation of this value in a measurement would directly point to physics beyond the SM (BSM).

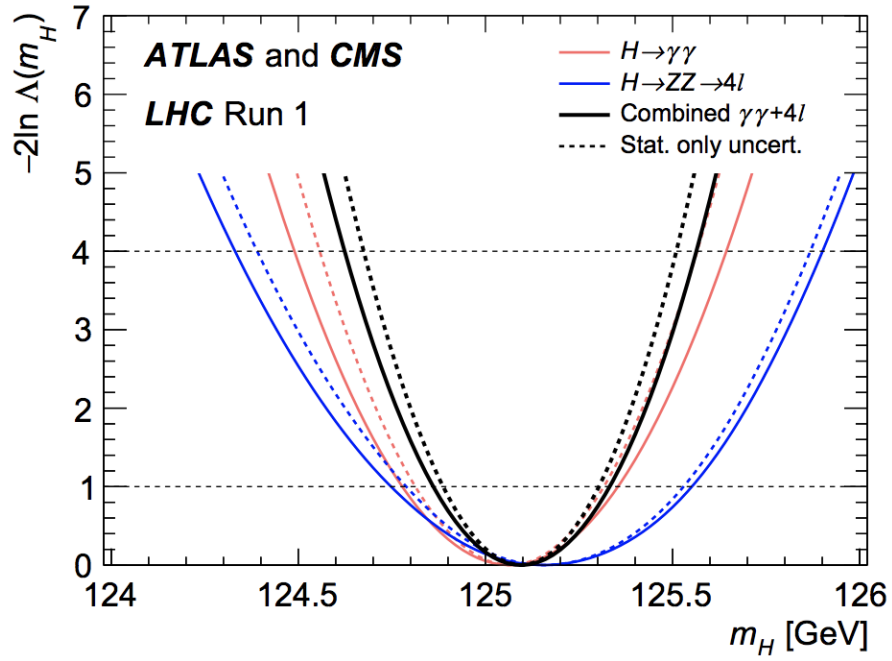


Figure 3.1: Combined likelihood fit of the Higgs boson mass by ATLAS and CMS [18].

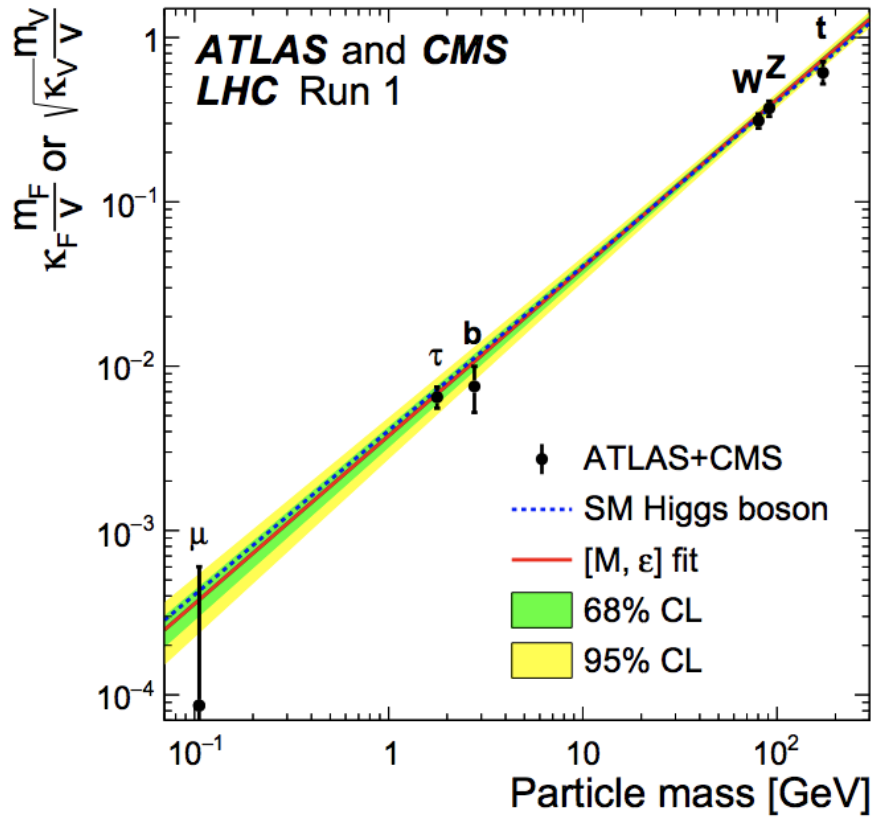


Figure 3.2: Higgs coupling to fermions or vector bosons as a function of the particle mass by ATLAS and CMS [18].

3.2 Exciting Times Ahead...

With the observation of a new scalar boson in July 2012 a milestone in particle physics was set. Now it is essential to measure all the properties of the Higgs boson with very high precision. Furthermore the Higgs boson can be used as a probe for new physics. Searches for dark matter produced in association with a Higgs boson are already ongoing. It is still not clear if there is only one Higgs boson or even more. Many BSM theories (like supersymmetry) require two Higgs doublets, which predict in total 5 Higgs bosons. Obviously these discoveries are only possible with upgrades in the experiments CMS and ATLAS and the accelerator LHC.

At LHC there is a future plan until 2035 to upgrade the experiment after Run 3 to a high luminosity machine (HL-LHC). The timetable is shown in figure 3.3.

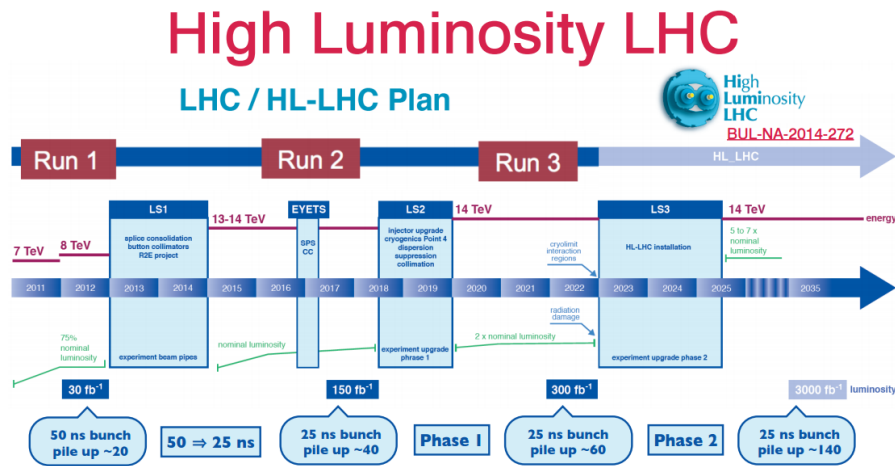


Figure 3.3: Future plan of LHC. A high luminosity upgrade is planned after Run3 until 2035 [19].

This upgrade will have some consequences. The main consequence is an increase in pile-up events, which makes data reconstructing even harder than before. Also an increased amount of data is very challenging for the trigger systems and storage systems.

A new experiment is currently planned in Japan, the so-called International Linear Collider (ILC). Its main purpose is to measure the mass, the interaction strengths and the CP properties of the Higgs boson with a very high precision. An accelerator of this kind is often referred to as a Higgs-factory.

All of these developments in Higgs physics will keep the future very interesting. New exciting results will definitely pop up in the near future.

Bibliography

- [1] CMS Collaboration, “Observation of a new boson at a mass of 125 GeV with the CMS experiment at the LHC”, *Phys. Lett. B* **716** (Jul, 2012) 30–61. 59 p.
- [2] ATLAS Collaboration, “Observation of a new particle in the search for the Standard Model Higgs boson with the ATLAS detector at the LHC”, *Phys.Lett.* **B716** (2012) 1–29, doi:tt10.1016/j.physletb.2012.08.020, arXiv:1207.7214.
- [3] P. Higgs, “Broken symmetries, massless particles and gauge fields”, *Physics Letters* **12** (1964), no. 2, 132–133, doi:tt10.1016/0031-9163(64)91136-9.
- [4] P. W. Higgs, “Broken Symmetries and the Masses of Gauge Bosons”, *Phys. Rev. Lett.* **13** (10, 1964) 508–509, doi:tt10.1103/PhysRevLett.13.508.
- [5] S. L. Glashow, “Partial-symmetries of weak interactions”, *Nuclear Physics* **22** (1961), no. 4, 579 – 588, doi:tt10.1016/0029-5582(61)90469-2.
- [6] S. Weinberg, “A Model of Leptons”, *Phys. Rev. Lett.* **19** (11, 1967) 1264–1266, doi:tt10.1103/PhysRevLett.19.1264.
- [7] A. Salam, “Weak and Electromagnetic Interactions”, *Conf.Proc.* **C680519** (1968) 367–377.
- [8] R. D. Ball et al., “Parton distributions with LHC data”, *Nucl. Phys.* **B867** (2013) 244–289, doi:tt10.1016/j.nuclphysb.2012.10.003, arXiv:1207.1303.
- [9] G. ’t Hooft and M. Veltman, “Regularization and renormalization of gauge fields”, *Nuclear Physics B* **44** (1972), no. 1, 189 – 213, doi:tthttps://doi.org/10.1016/0550-3213(72)90279-9.
- [10] LHC Higgs Cross Section Working Group et al., “Handbook of LHC Higgs Cross Sections: 1. Inclusive Observables”, *CERN-2011-002* (CERN, Geneva, 2011) arXiv:1101.0593.
- [11] LHC Higgs Cross Section Working Group et al., “Handbook of LHC Higgs Cross Sections: 2. Differential Distributions”, *CERN-2012-002* (CERN, Geneva, 2012) arXiv:1201.3084.
- [12] LHC Higgs Cross Section Working Group et al., “Handbook of LHC Higgs Cross Sections: 3. Higgs Properties”, *CERN-2013-004* (CERN, Geneva, 2013) arXiv:1307.1347.
- [13] CMS Collaboration, “Observation of a new boson at a mass of 125 GeV with the CMS experiment at the LHC”, *Phys. Lett. B* **716** (Jul, 2012) 30–61. 59 p.

-
- [14] ATLAS Collaboration, “Observation of a new particle in the search for the Standard Model Higgs boson with the ATLAS detector at the LHC”, *Phys.Lett.* **B716** (2012) 1–29, doi:tt10.1016/j.physletb.2012.08.020, arXiv:1207.7214.
- [15] “Measurement of inclusive and differential cross sections in the H to ZZ to 4l decay channel in pp collisions at a center-of-mass energy of 13 TeV with the ATLAS detector”, *Journal of High Energy Physics* **2017** (Oct, 2017) 132, doi:tt10.1007/JHEP10(2017)132.
- [16] CMS Collaboration, “Measurements of properties of the Higgs boson in the four-lepton final state at a center-of-mass energy of 13 TeV”, 2018. Currently @ pre-approval. Not public yet!
- [17] CMS Collaboration Collaboration, “Observation of the SM scalar boson decaying to a pair of τ leptons with the CMS experiment at the LHC”, Technical Report CMS-PAS-HIG-16-043, CERN, Geneva, (2017).
- [18] R. Wolf and A. Gilbert, 2014.
<http://ekpwww.physik.uni-karlsruhe.de/~rwolf/teaching/ss16/Higgs-VL-14-HiggsCouplings.pdf>.
- [19] 2015. HL-LHC: <http://francis.naukas.com/2015/06/02/primera-semana-de-haces-estables-y-colisiones-de-protones-en-el-lhc/>.